JOURNAL OF MATERIALS SCIENCE **38** (2003) 1139–1145

A comparative study of the electrochemical behaviour of Algerian zinc and a zinc from a commercial sacrificial anode

M. BOUNOUGHAZ
SONATRACH—Centre de Recherche et Développement

E. SALHI
Ecole Nationale Polytechnique d'Alger

K. BENZINE
SONATRACH—Centre de Recherche et Développement

E. GHALI
Département des Mines et Métallurgie, Université LAVAL, Quebec, Canada

F. DALARD
LEPMI, Institut National Polytechnique GRENOBLE, BP 75, 38402 Saint Martin d'Hères, France

Zinc is used in the oil industry as a sacrificial anode for protecting steel storage tanks from corrosion. The behaviour of a sample of zinc from the Algerian metallurgy industry (zinc A) and a commercially available zinc (zinc B) was compared in an electrolyte from storage tank drainage water. The corrosion potential measurements for zinc A confirmed that this material could be used as a sacrificial anode. The polarization curves of the two materials (zinc A and zinc B) were different, zinc A being the least polarized. Thus, the same corrosion protection could be obtained with a lower surface ratio (S_{Zn}/S_{Fe}) for Zinc A. Cyclic voltammetry curves provided evidence of a surface layer formed by dissolution products. To provide protection over extended periods of time, the zinc anode must be oversized. The two types of zinc tested were comparable.

The results of the impedance spectroscopy study confirmed the previous results. The corrosion layer formed on zinc A was not prejudicial to dissolution. Hence, the properties of this zinc were found to be satisfactory for its use as a sacrificial anode.

1. Introduction

Crude oil conveyed to storage tanks generally contains non-negligible amounts of water. This decanted water is most often contaminated by sulfate reducing bacteria (SRB). Although the bottoms of carbon steel storage tanks are epoxy resin coated, corrosion is initiated in the defects in the coating and is accelerated by the SRB. Eventually, holes may form in the bottom of the tanks, resulting perforation of the tank wall and in pollution of the site. To avoid such situations, zinc sacrificial anodes are used to improve tank bottom protection. Coupling of the zinc sacrificial anodes to the carbon steel structure shifts the corrosion potential of the steel towards cathodic values [1, 2]. The carbon steel will then be in its immunity range and will no longer corrode. Zinc sacrificial anode consumption depends on the surface areas to be protected and the quality of the epoxy coating.

Aluminium, magnesium and zinc are used as sacrificial anodes for protecting submerged steel structures. These metals all have very negative potentials. Galvanic coupling between the steel structure to be protected and the anode (Al, Mg or Zn) accelerates corrosion (dissolution) of the anode. The amount of current needed to protect the metal structure determines the mass of the sacrificial anode to be used. The galvanic coupling current density is also dependent on the protective potential as well as on numerous factors such as the hydrodynamic conditions, temperature, dissolved oxygen concentration, bacterial activity and the quality of the tank bottom coating [3–5].

When a steel structure is cathodically protected, oxygen reduction is promoted and the surrounding environment becomes more alkaline. As a result, the solubility of calcium and magnesium carbonates is reduced and precipitates are formed on the cathodic sites. This favours a reduction in the amount of current required for protection and also makes it possible to reduce sacrificial anode consumption [6, 7].

The distribution of the sacrificial anodes over the entire surface to be protected must be carefully calculated. The parts of the steel structure at some distance from the sacrificial anode may not receive adequate protection,

while the metal surfaces close to the anode may receive too much protection. Excessive protection results in hydrogen evolution, which causes damage to the protective coating [9–11].

Electrochemical studies were performed on zinc produced by the Ghazaouet facility in Algeria (Zinc A) to determine its performance as a sacrificial anode for protecting the inside of storage tanks. The chemical analyses and electrochemical behaviour were compared with those of a sacrificial anode made of commercially available zinc (Zinc B). The polarization tests, corrosion potential measurements and impedance measurements were performed in drainage water removed from a storage tank. Our aim was to be able to recommend the use of zinc A for sacrificial anodes in the Algerian oil industry.

2. Experimental methods

2.1. Electrodes

The chemical composition of the zinc specimens A and B was determined using X-ray fluorescence spectrometry. The results are shown in Table I.

Material A was composed essentially of two elements, namely zinc (98.8%) and aluminium (1.06%). The zinc content of material B was 99.2%.

Trace elements of iron were found in Material A, at a concentration of less than 10 ppm, while in material B the concentration was 0.073%. The iron content must be low since this element is conducive to enhanced self corrosion of the zinc and causing it to deliver less current.

Trace elements of lead were found in Material A (concentration of less than 10 ppm), while in material B the lead concentration was 0.016%.

The working electrodes used for the electrochemical measurements were circular, 10 and 8 mm in diameter respectively for material A and material B, and were coated with a thermosetting resin. The working electrodes were mechanically polished with wet abrasive paper of increasingly finer grit (up to 1200 mesh). After polishing, the electrodes were washed in water, then rinsed with acetone and used immediately.

2.2. Electrolyte

The electrochemical measurements were performed at $25 \pm 1^{\circ}$C in drainage water taken from an oil storage tank. The chemical composition of this water is given in Table II.

TABLE I Chemical composition of the experimental materials

Element (%)	Al	S	Ti	Fe	Zn	Pb
Zinc A	1.06 ±0.05	0.008 ±0.002	0.0066 ±0.0006	<10 ppm	98.8 ±2.3	<10 ppm
Zinc B	0.58 +0.03	<10 ppm	0.0078 ±0.0007	0.073 ±0.006	99.2 ±2.3	0.016 ±0.003

TABLE II Chemical composition of drainage water

Element	Ca^{++}	Mg^{++}	Fe^{2+}	Na^{+}	K^{+}	Cl^{-}	SO_4	NO_2^-
c ($mg \cdot L^{-1}$)	230.83	45.00	7.02	400.17	7.67	678.47	2.08	3.58

2.3. Electrochemical set-up

The electrochemical set-up comprised an EGG (PAR 273A) digital potentiostat and a Solartron 1255 frequency response analyser. Zplot and Zview software from Solartron and EGG M352 were used for data acquisition and processing.

3. Results and discussion

3.1. Corrosion potential

The changes in the corrosion potential of the two sacrificial anode materials (Zinc A and B) over time are illustrated in Fig. 1.

The corrosion potential of Zinc A increased over time from an initial value of −1070 mV/SCE and stabilised after 4000 sec immersion. The potential reached was of the order of −1046 mV/SCE.

The initial corrosion potential measurement for zinc B was −1083 mV/SCE. It reached a stationary value of −1053 mV/SCE after 4000 seconds. After about 2 hours, the behaviour of both of the zinc samples was comparable.

For a given surface ratio (S_{Zn}/S_{Fe}), it should be possible, by coupling Zinc A to a metal structure, to reach a protective potential similar to that obtained in the presence of Zinc B.

3.2. Linear potential scan voltamperometry

The polarization curves obtained with these electrodes are shown in Fig. 2.

Two characteristics can be observed from the voltammograms for zinc A (Fig. 3). The first is the low polarization of the electrode at potential values around −1000 mV/SCE and for current densities below 0.4 $\mu A \cdot cm^{-2}$. The second characteristic is that the dissolution current density is independent of the applied potential, in the potential range above −500 mV. Its limiting value is around 0.5 $\mu A \cdot cm^{-2}$. A corrosion layer ("salt film") was formed on the surface of the electrode at this current. The voltammogram for material B is characterized by a greater increase in polarization in the potential range above −1000 mV/SCE and for current densities below 0.3 $\mu A \cdot cm^{-2}$. The current density of zinc A was greater than that recorded in the presence of material B at all anodic potentials.

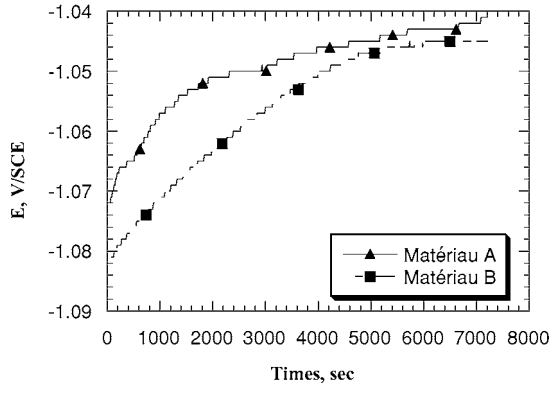

Figure 1 Variation in corrosion potential of zinc in drainage water from storage tank zinc A (▲), zinc B (■).

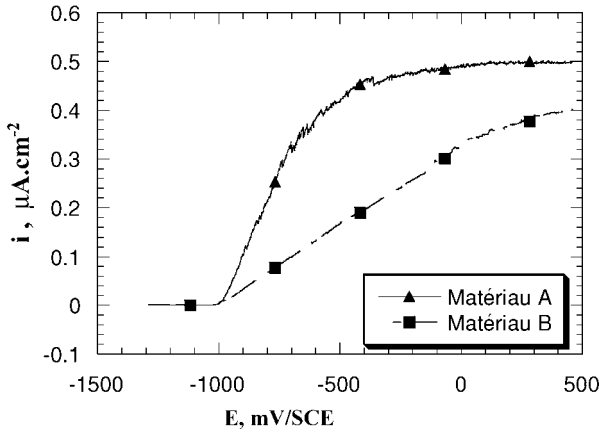

Figure 2 Voltammogram of zinc in drainage water. Scanning rate $v_b = 5\ mV \cdot s^{-1}$. Zinc A (▲), zinc B (■).

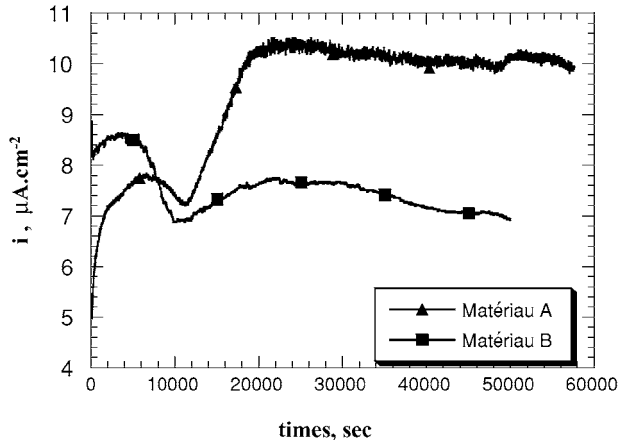

Figure 3 Current density vs. times. Applied potential $E_{app} = E_{corr} + 10$ mV.

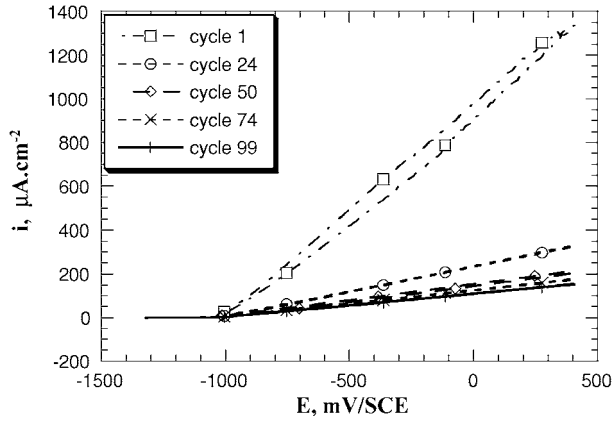

Figure 4 Zinc A, polarization curves vs number of cycles. Scanning rate $v_b = 5\ mV \cdot s^{-1}$.

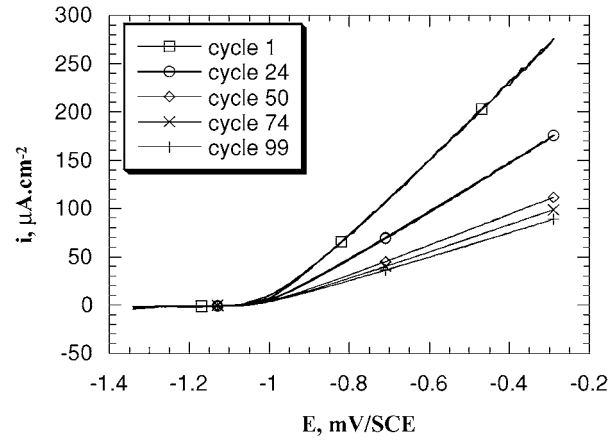

Figure 5 Zinc B, polarization curves vs number of cycles. Scanning rate $v_b = 5\ mV \cdot s^{-1}$.

Thus, when the zinc was coupled to a metal structure, the same protective potential was obtained with a lower surface ratio (S_{Zn}/S_{Fe}) for zinc A than per zinc B.

The zinc electrodes (zinc A and zinc B) were polarized at a slightly anodic potential compared with the corrosion potential, namely $+10$ mV/E_{corr}. Changes in the oxidation current density versus immersion time are illustrated in Fig. 3. These results confirm the characteristics shown in Fig. 2.

For short times ($t < 8000$ s), the activity of material A was lower than that of material B. For longer times, the opposite was observed. The oxidation current of material A was around 10 $\mu A \cdot cm^{-2}$ while that of material B was around 7 $\mu A \cdot cm^{-2}$. The variations in current density over time must be caused by the formation of oxidation products. This layer would tend to slow down ($t = 10000$ s) the zinc dissolution, but not prevent it.

In order to test the behaviour of the zinc electrodes, cyclic voltammograms were obtained for each specimen (Figs 4 and 5). The curves were obtained at a potential scan rate of 5 mV/s and for a hundred cycles for each zinc electrode.

The dissolution current densities were higher with zinc A for the first cycle. The dissolution current densities decreased with the number of cycles (zinc A and zinc B).This drop could be due to an accumulation of dissolution products on the surface of the zinc (corrosion products) [11]. Thus, the efficiency of the zinc electrodes decreased during the cycling. The anode surface intended to protect a given surface area of steel must therefore be oversized. This phenomenon was the same for both materials.

3.3. Impedance measurements

The measurements were performed at corrosion potential for the two zinc specimens after different immersion times. (The linearity and stationary state of the system was checked). The impedance diagrams are shown in Nyquist (and Bode) form.

With zinc A (Fig. 6), the impedance diagrams varied as a function of immersion time. Two capacitive semi circles can be distinguished (high frequency and low frequency) and an inductive semi circle at very low frequency. Low frequency resistance increased from 180 to 200 $\Omega \times cm^2$ when the immersion time increased from 1 hr to 2 hr. This increase in resistance may be attributed to the presence of corrosion products on the surface of the material.

For longer immersion times, the low frequency resistance dropped regularly from 200 to 50 $\Omega \times cm^2$. This change may be attributed to an increase in the real surface (increase in surface roughness) of the specimen. The high frequency part of the second semi circle appears more clearly with longer experimental time. This change is consistent with the formation of corrosion products.

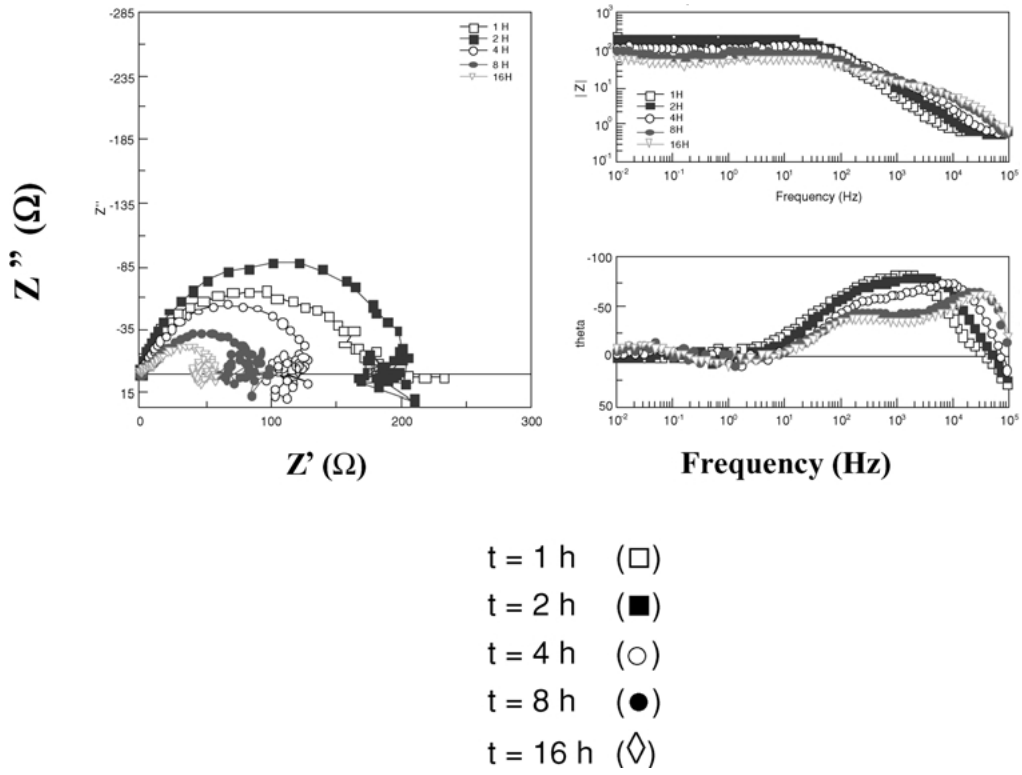

Figure 6 Zinc A, electrochemical impedance spectroscopy at different immersion times. Measurements performed at corrosion potential. Nyquist and Bode diagrams.

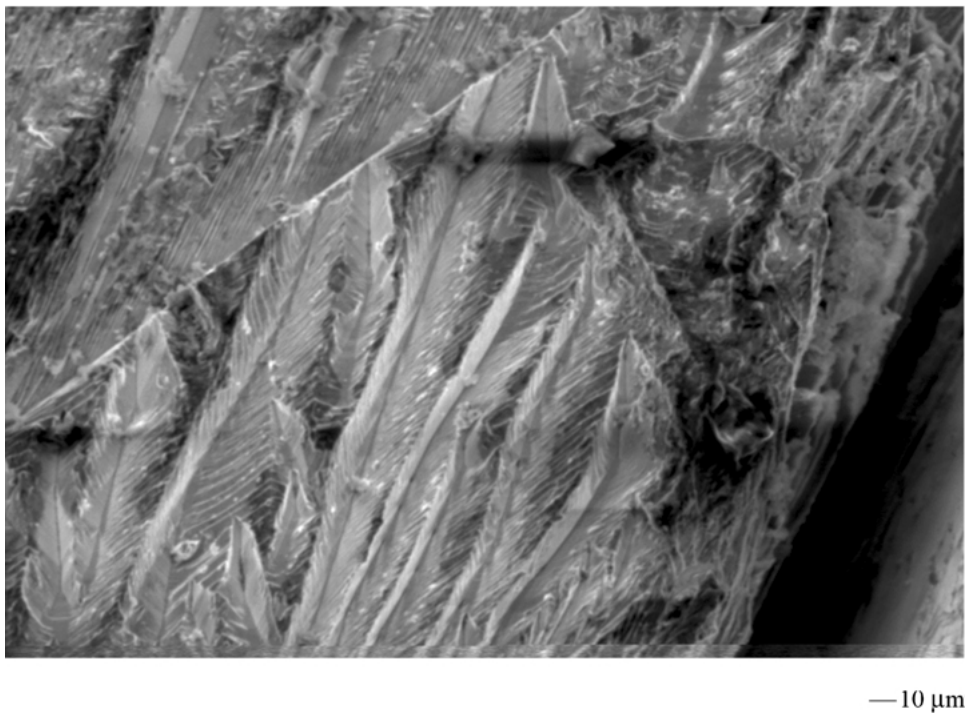

Figure 7 Zinc A, SEM micrograph after 16 h immersion in drainage water.

The SEM micrograph of the specimen surface after 16 hr of immersion at corrosion potential confirms the formation of a deposit on the surface of the metal (Fig. 7).

At very low frequencies, an inductive loop can be observed, probably due to the formation of Zn^{+}. The high frequency resistance did not vary, and can be estimated at 0.5 $\Omega \times cm^2$. This value corresponds to the resistance of the electrolyte.

With zinc B, the impedance diagrams (Fig. 8) also varied as a function of immersion time and have a similar appearance to those of material A. The low frequency resistance was lower than that of zinc A, and dropped regularly from 30 to 12 $\Omega \times cm^2$. This variation could be attributed to an increase in the real surface area (increase in the surface roughness) of the specimen. The high-frequency part of the semi circle is consistent with the formation of corrosion products.

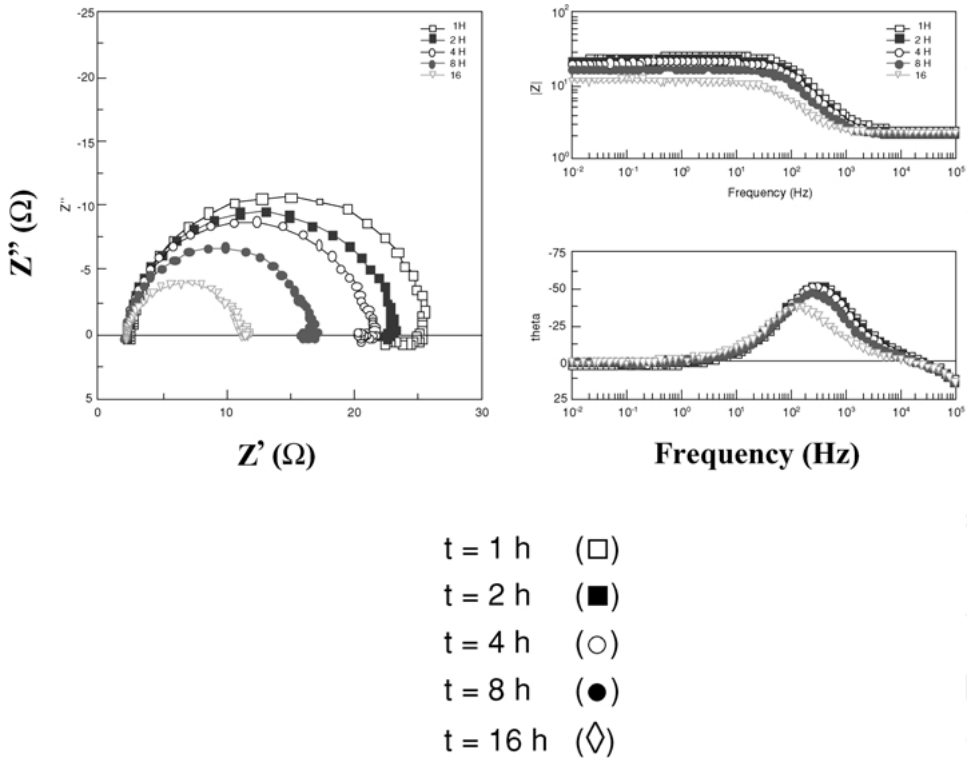

Figure 8 Zinc B, electrochemical impedance spectroscopy at different immersion times. Measurements performed at corrosion potential. Nyquist and Bode diagrams.

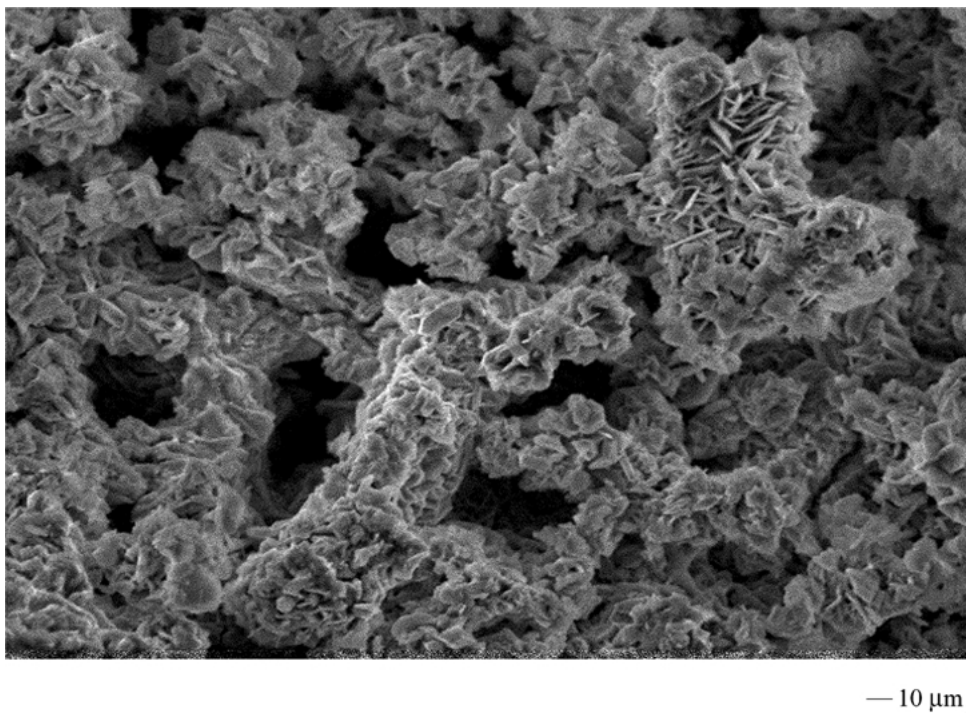

Figure 9 Zinc B, SEM micrograph after 16 h immersion in drainage water.

The SEM micrograph of the specimen surface after 16 hr of immersion at corrosion potential confirmed the formation of a deposit on the surface of the metal (Fig. 9). At very low frequencies, an inductive loop was also observed, corresponding to the formation of Zn^+. The high frequency resistance did not vary, and can be estimated at 2 $\Omega \times cm^2$, which corresponds to the resistance of the electrolyte. The developed surfaces of the two specimens were different, that of zinc B differing by a factor of 4 from zinc A.

The results obtained by EIS are in agreement with the results shown in Fig. 3. Zinc A, for short immersion times, corroded less than zinc B, the dissolution current density being lower for this specimen.

To complete our results, we performed the same EIS measurements at potential $E = E_{corr} + 10$ mV.

The curves obtained were of a similar shape, with a capacitive part and an inductive part. The very low frequency inductive part likely due to the formation of an adsorbed layer of Zn^+ speries was confirmed with

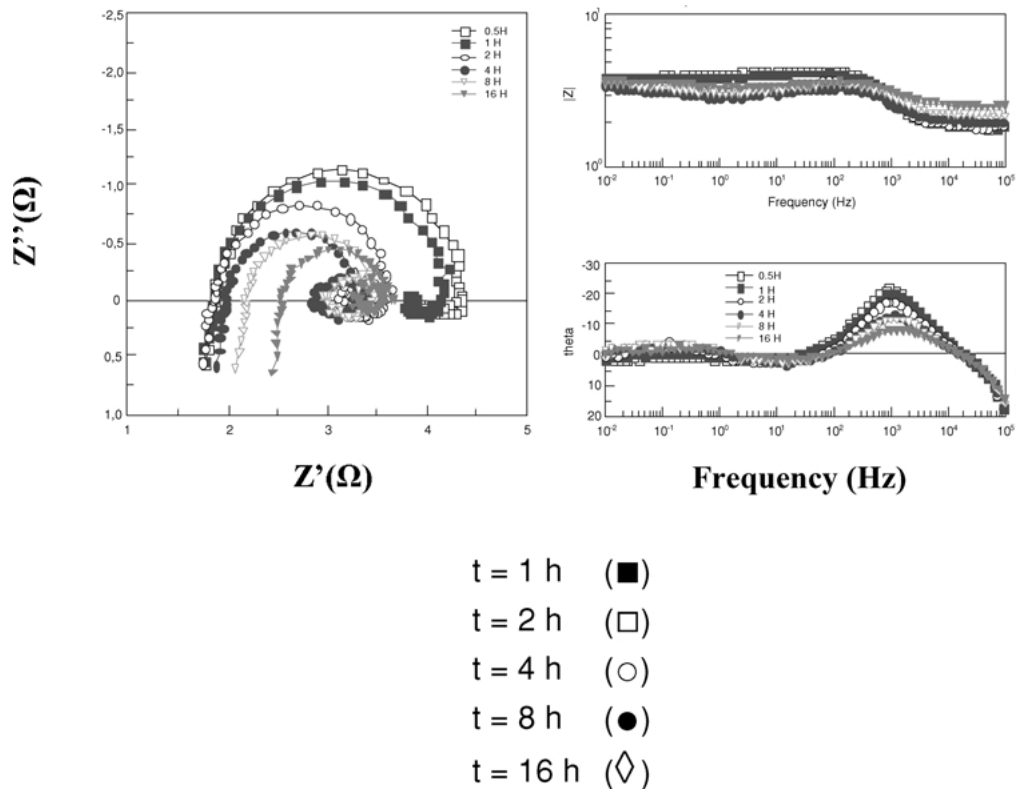

Figure 10 Zinc A, electrochemical impedance spectroscopy at different immersion times. Nyquist and Bode diagrams. Measurements performed at $E = E_{corr} + 10$ mV.

both zinc specimens. The two capacitive semi circles (high frequency) are difficult to distinguish.

With zinc A, (Fig. 10), the impedance diagrams varied with immersion time. The low frequency resistance decreased regularly from 4.4 to 3.2 $\Omega \times cm^2$ when immersion time was increased from 0.5 hr to 16 hr. This value was lower than the previous measurements. The dissolution of zinc A eliminated the corrosion products on the surface of the metal. It was thus not surprising that it was more difficult to identify the influence of the corrosion products (high frequency semi circle) and easier to identify the presence of Zn^+,

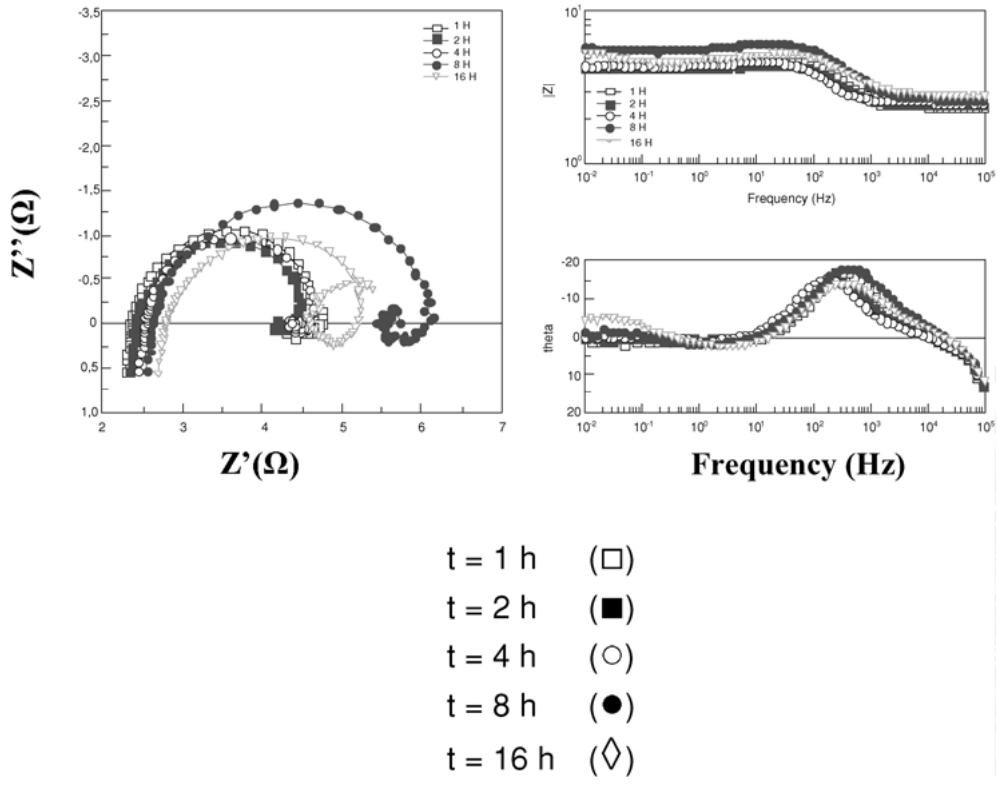

Figure 11 Zinc B, electrochemical impedance spectroscopy at different immersion times. Nyquist and Bode diagrams. Measurements performed at $E = E_{corr} + 10$ mV.

ads. The resistance of the electrolyte was estimated at $2\ \Omega \times cm^2$.

With zinc B, (Fig. 11), the impedance diagrams varied as a function of immersion time. The low frequency resistance dropped initially and decreased from 5.2 to $4.8\ \Omega \times cm^2$ between 1 hr and 2 hr of immersion. It then started to increase, reaching a value of $6.3\ \Omega \times cm^2$ after 16 hr immersion. These values are lower than those measured at corrosion potential. The dissolution of the zinc remained related to the formation of corrosion products. The resistance values of zinc B during dissolution were higher than those of zinc A. This result is consistent with Fig. 3 where the dissolution current for zinc A is highest for long time periods. The resistance of the electrolyte was again estimated at $2\ \Omega \times cm^2$.

The EIS measurements showed that zinc grade A corroded less than grade B at corrosion potential. Dissolution was easier in the case of specimen A than specimen B. It is therefore possible to envisage using zinc A as sacrificial anode in this electrolyte.

4. Conclusions

1. The corrosion potential of the two specimens of zinc, Algerian zinc (zinc A) and commercially available zinc (zinc B), were compared. In both cases, this potential was sufficiently low for the zinc to be used as a sacrificial anode to prevent corrosion of steel crude oil storage tanks.

2. The voltammetry curves showed that, over long time periods, zinc A was easier to oxidize, the current density values being higher at equivalent potential values.

3. The impedance spectroscopy results confirmed that the corrosion layer formed on zinc A provided greater protection. But when there was dissolution of the zinc, this layer did not cause passivation of the specimen.

4. Thus, both materials tested can be used as sacrificial anodes to protect the bottom of storage tanks against corrosion but the greater effectiveness is with zinc A .

References

1. R. BROUSEAU, *Construction Canada*, **35**(5) (1992) 29.
2. Steel Tank Institute, Optional Recommended Practice for Control of Localized Corrosion Within Underground Steel Petroleum Storage Tanks, R 831–98, STI, November 16, 1998.
3. J. PERKINC, W. H. LUEBKE, J. K. GRAHAM and J. M. TODD, *J. Electrochem. Soc.* **124** (1977) 819.
4. R. J. KESSLER and R. G. POUWERS, in Corrosion 90, 1990, paper no. 324.
5. K. P. FISHER, *Materials Performances* **20** (1981) 41.
6. K. P. FISHER, in *15th Annual OTC in Houston*, Texas, May 2–5, 1983, p. 451.
7. R. U. LEE and J. R. AMBROSSE, *Corrosion (NACE)* **44** (1988) 887.
8. W. H. HARTT and S. CHEN, *ibid.* **55** (1999) 596.
9. E. SCHASCHL and G. A. MARSH, *Materials Performance*, **13** (1974) 9.
10. T. J. BARLO, *Pipeline Technology*, ASME **5** (1995) 285.
11. S. C. CHUNG, A. S. LIN, J. R. CHANG and H. C. SHIH, *Corros. Sci*. **42** (2000) 1599.

Received 5 June
and accepted 31 October 2002